https://doi.org/10.1016/j.jclepro.2021.127082

Effects of Rubber Absorption on the Aging Resistance of Hot and Warm Asphalt Rubber Binders Prepared with Waste Tire Rubber

Danning Li[a], Zhen Leng[a*], Fuliao Zou[a], Huayang Yu[b]

[a] Department of Civil and Environmental Engineering Department, The Hong Kong Polytechnic University, Kowloon, Hong Kong

[b] School of Civil Engineering and Transportation, South China University of Technology, 510641, Guangzhou, China

[*]Corresponding author: Zhen Leng, Tel: +852-2766-6007; Fax: 852-2334-6389; Email: zhen.leng@polyu.edu.hk

ABSTRACT

Recycled from waste tires, crumb rubber modifier (CRM) is added into bitumen to produce the asphalt rubber (AR) with superior performances but a more complex aging mechanism. With much attentions paid to the complex composition of CRM, the effect of rubber absorption on the aging resistance of AR remains unclear, especially when warm mix asphalt (WMA) technology is combined. Therefore, this study aims to investigate the role of CRM absorption in improving the aging resistance of AR and warm asphalt rubber (WAR) binders. One AR and two WAR binders were prepared, as well as a direct mixing-AR (DAR) binder, which did not have significant CRM absorption, for comparison. The prepared binders under different aging conditions were separated into binder liquid phases and absorbed gel layers for various chemical and rheological analyses. Chemical characterization indicated that CRM could hinder the attack of oxygen on bitumen, and the absorbed fractions in the gel layers were less oxidized after aging. During aging, the rubber tended to preserve the light fractions inside the gel layer and expel the large molecules into the liquid phase, which maintained the relatively softer environment around the swelling rubber. Furthermore, the contribution of rubber absorption to the aging resistance was reflected by the less changed rheological properties of AR compared with the raw bitumen and DAR. The incorporation

of WMA additives affected the rheological properties of AR but the aging resistance is not compromised. Overall, it was concluded that sufficient rubber absorption should be emphasized during the production of AR for better aging resistance, and the use of WMA additives can be considered for a more environmental-friendly production.

Keywords: Waste tire rubber recycling, Aging resistance, Warm asphalt rubber, Rubber absorption, Rheological property, Chemical analysis

1 Introduction

With the ever-increasing number of vehicles, the disposal of waste tires has become an urgent environmental issue. While being the "black pollution" to the environment, waste tires are also abundant and inexpensive polymer resources (Kabir et al., 2021). Crumb rubber modifier (CRM) ground from waste tires has been widely applied as a bitumen modifier for over 50 years. Adding CRM into bitumen not only extends the service life of asphalt pavement but also replace part of the bitumen, which is considered a sustainable way to recycle the waste tires and reduce the need for natural bitumen resources (Milad, et. al., 2020; Shu and Huang, 2014). Wet-process Asphalt Rubber (AR) is one of the approaches to incorporate CRM into hot mix asphalt (HMA) where the dosage of CRM is more than 15wt% of the raw bitumen (ASTM-D6114, 2009). The enhanced rutting and fatigue resistances of AR compared with raw asphalt binder have been well documented and widely acknowledged (Presti, 2013; Wang et al., 2018b). However, the poor workability of AR due to its high viscosity has also been criticized since the preparation and construction of AR require higher energy consumption and produce more emissions of greenhouse gas and volatile organic compounds (Wang et al., 2018d). To address this issue, various warm mix asphalt (WMA) technologies have been adopted to produce warm asphalt rubber (WAR) mixtures, which helps to decrease the viscosity of AR, thus reducing the production temperature by 15-30 ^{o}C (Wang et al., 2018c). The incorporation of WMA additives improves the workability of AR and allows for more energy saving and emission reduction during the production and paving process (Yu et al., 2020a).

Therefore, WAR has now become a popular sustainable paving technology because of its balanced pavement performance and environmental effects.

Aging of bitumen is an inevitable process in the long-term service of pavement, which includes the oxidative reactions, volatilization of light fractions, and transformation of aromatics and resins to asphaltenes (Lesueur, 2009). The aging occurs faster during summer due to the more active diffusion of oxygen at higher temperature. The ascending concentration of oxygen-containing functional groups enlarges the molecular weight and strengthens the intermolecular association inside of bitumen, resulting in immobilization of bitumen molecules under mechanical and thermal stresses (Moraes and Bahia, 2015). Mechanically, bitumen gains more stiffness and loses certain relaxation capacity after long-term aging, which makes bitumen more brittle and vulnerable to cracking during the low-temperature season (Rahbar-Rastegar et al., 2018).

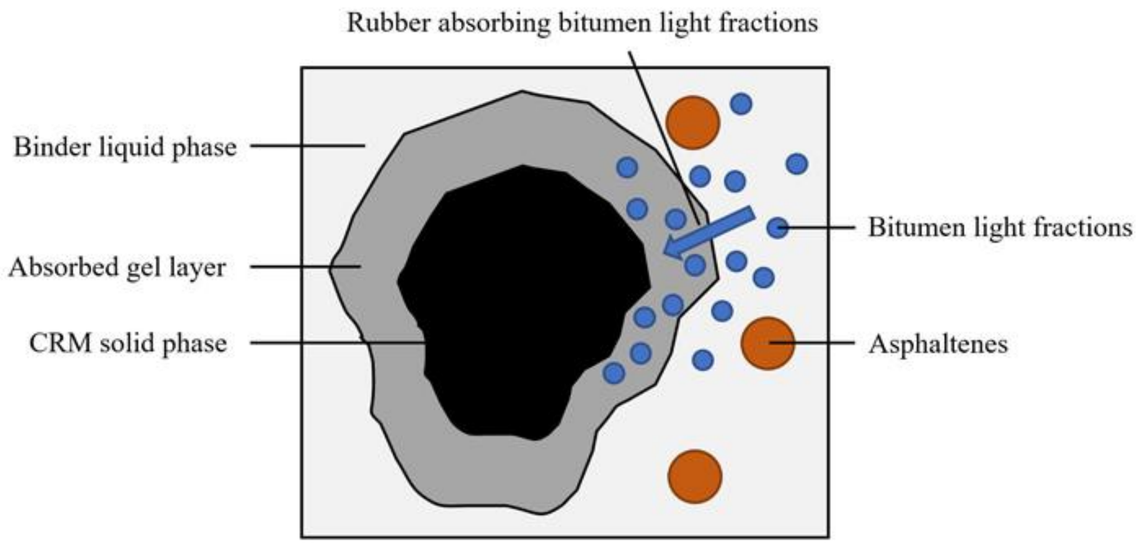

Fig. 1. Schematic of rubber absorption and swelling

As more and more AR pavement are put into application around the world, its unclear recyclability at the end of its service life has become a major concern due to the insufficient understanding of its aging mechanism. The recycling of waste tires in bitumen modification provides numerous economic and environmental benefits, but it also complicates the aging mechanism of bitumen. The addition of CRM into bitumen has been reported to enhance the aging resistance, supported by the fact that AR showed lower carbonyl and sulfoxide indexes and less changed rheological parameters after laboratory aging compared with raw bitumen (Wang et al., 2020c). To investigate the role of CRM in improving the aging resistance of bitumen, many researchers focused on the complex composition of CRM itself. Taking up most of the composition, the rubber polymers in CRM degrade during aging, which is believed to improve the aging resistance of AR by attenuating the mechanical properties of the binder and offsetting the hardening effect of bitumen aging (Wang et al., 2020c; Tang et al., 2016). In addition, Ouyang et al. (2006) and Wang et al. (2019) have found that additives in CRM, i.e., carbon black and antioxidants could hinder the intrusion of oxygen into bitumen molecules. However, most of the literature has overlooked the absorption behavior of rubber when exploring the aging mechanism of AR. When CRM is added to and mixed with bitumen at high temperature, the rubber swells by absorbing light fractions from bitumen, which transforms bitumen into a multiphase system composed of the binder liquid phase, the CRM solid phase, and the gel layer between them, as illustrated in Fig. 1 (Ghavibazoo and Abdelrahman, 2013; Wang et al., 2020b; Wang et al., 2018a). The absorption behavior of CRM alters the distribution of bitumen fraction. The light bitumen fractions stored in the gel layer may react differently during aging process from those in the binder liquid phase and those in raw bitumen, but so far very limited research has been conducted to quantitatively verify such differences.

Aiming at a deeper and more comprehensive understanding of the aging behavior of AR and WAR binders, one AR binder, two WAR binders (with wax-based and chemical WMA additives), and one direct mixing-AR (DAR) binder where only minimal rubber absorption occurred, were prepared. Self-developed separating methods were used to extract the liquid phases and absorbed gel layers from these AR and WAR binders for more detailed analyses. A series of chemical and rheological tests were conducted on the AR and WAR binders and their components under different aging conditions. The mechanical evolutions of AR and WAR binders and the composition changes of their liquid phases and gel layers during aging were combined to disclose the contribution of rubber absorption to the enhanced aging resistance and the influences of WMA additives. It is expected to provide theoretical support for the longer service life of AR pavement, the use of WMA additives, and the recycling and rejuvenation of reclaimed AR pavement.

2 Experimental Program

2.1 Materials and sample preparation

The raw materials used for preparing AR binders were raw bitumen with a penetration grade of 60-70 (Pen60/70) commonly used in Hong Kong and 40-mesh CRM produced from ambient grind. AR binders were produced by using a high shear mixer to incorporate CRM (20% by weight of the raw asphalt) into raw asphalt binder at 180 ^{o}C and a speed of 4000 rpm for one hour. This is considered as the wet process where sufficient rubber swelling and absorption were achieved. To highlight the influence of rubber absorption, a Direct mixing-AR (DAR) binder was prepared as a matched group, where the CRM was simply dispersed in raw asphalt with minimal formation of gel layer. The DAR was produced by using a glass stick to manually stir CRM into Pen60/70 at different aging conditions for 3 min at 165 ^{o}C until evenly distributed. In addition, one wax-based WMA additive and one chemical WMA additive were used to produce WAR binders with the dosages of 3wt% and 5wt% recommended by the producers, respectively. Table 1 shows the basic properties of these two WMA additives. The wax-based additive shows a solid lattice structure at ambient temperature, but it melts into liquid at mixing temperature to reduce the viscosity of AR (Yu et al., 2019; Xiao et al., 2012). As for the chemical additive, its surfactant composition can reduce the friction between bitumen and CRM particles (Xiao et al., 2012; Yu et al., 2020c). Therefore, the WAR binders were produced by mixing WMA additives with raw asphalt and same content of CRM by high shear mixer at 160 ^{o}C and 4000 rpm for one hour. Meanwhile, AR mixed with wax-based and chemical additives were nominated as ARW and ARC, respectively. The preparation parameters of AR and WAR binders used in this study have been proved to obtain satisfied rheological properties in previous work (Wang et al., 2018; Yu et al., 2020b).

TABLE 1 Basic properties of WMA additives

WMA additives	Wax-based	Chemical
Ingredients	saturated hydrocarbons	fatty amine derivatives, alkylamines
Dosage	3wt% of AR binder	5wt% of AR binder
State	solid	liquid
Color	milk white	amber
Odor	none	amine-like
Density	0.622 g/cm^3	1.0-1.1 g/cm^3
PH value	N/A	9-10
Melting point	105-110 ^{o}C	N/A
Boiling point	N/A	150-170 ^{o}C
Water solubility	insoluble	partially soluble

2.2 Laboratory aging procedure

Aging of bitumen can be divided into short-term aging and long-term aging. Short-term aging refers to the rapid oxidation of bitumen at high temperature during the construction stage, which is normally simulated by the rolling thin film oven (RTFO) test in the laboratory. However, there are some limitations when RTFO is applied to AR, because the AR binder does not own enough flowability to evenly coat the inside wall of the bottle due to its high viscosity, which significantly impairs the aging effect. Moreover, it is hard to get AR out of the bottle after the RTFO test. To address these difficulties, Wang et al. proposed a two-hour thin film oven (TFO) test as an alternative method for the standard RTFO test, where similar aging levels can be achieved between the two tests for raw bitumen (Wang et al., 2020c). In the TFO test, 20 g of bitumen sample was poured onto a 140 mm-diameter pan to make a thin film of 1.25 mm thickness and the pan was placed in an oven of 163 ^{o}C with a static shelf instead of the rolling rack. Long-term aging refers to the progressive oxidation of bitumen during the service stage of asphalt pavement. After the samples were subjected to the TFO short-term aging test, the binders were further conditioned by the pressure aging vessel (PAV) test to simulate the long-term aging effect. 50 g of TFO-aged binder sample was poured onto a 140 mm-diameter pan with a film thickness of 3.2 mm. The pan was then stored in a vessel with a pressure of 2.1 ± 0.1 MPa at 100 ^{o}C for 20 and 40 h to simulate different long-term aging levels. In the end, binders under four aging conditions were prepared, including unaged, TFO-aged, 20-hour PAV-aged, and 40-hour PAV-aged. The corresponding binders are labelled as UN, TFO, PAV, and 2PAV, respectively, in this study.

2.3 The extraction of asphalt liquid phase and absorbed gel layer

Since a precise analysis on the anti-aging mechanism of rubber absorption is the primary purpose of this study, AR and WAR binders under different aging conditions were separated into binder liquid phases, absorbed gel layers, and CRM solid phase. Binder liquid phase was first separated from swelling CRM particles by using the separating system as shown in Fig. 2(a). The separating system is composed of a 200-mesh (0.075 mm) sieve, a metal container, and a cap for sealing the sieve to reduce the contact of binder with air. 15 g of AR/WAR binders at different aging conditions were poured onto the sieve and then the whole system was stored in an oven of 165 ºC for 20 min. Inside the oven, the binder liquid phase could flow through the sieve pore and fall into the container, leaving the swelling CRM particles on the sieve. After the separation process, no liquid binder could be observed at the lower side of the sieve, which represented a good separation between swelling rubber and binder liquid phase. The binder liquid phase in the container was then collected for weighing and chemical tests. To eliminate the possible influence of extra aging during the separation process, the same heating process was conducted on raw bitumen at different aging conditions before the chemical tests.

The swelling CRM particles on the sieve were removed for the extraction of gel layer. Less than 10 g of swelling CRM particles were wrapped inside a piece of 200-mesh sieve net and immersed into a beaker filled with 80 ml of dichloromethane (DCM) solvent, as shown in Fig. 2(b)&(c). The selection of DCM was supported by preliminary tests. Thermal Gravimetric Analysis (TGA) and Fourier Transform Infrared Spectroscopy (FTIR) tests were conducted on raw CRM particles and CRM particles that have been soaked in DCM solvent for 24 hours. The TGA results showed that the ratios of natural rubber (NR), synthetic rubber (SR), and carbon black plus inorganics (CB+IN) barely changed from 44.72%, 18.27%, and 37.01% to 45.16%, 18.05%, and 36.79%, respectively (3 replicates). Meanwhile, the FTIR results showed no change of functional groups in CRM after soaking in DCM solvent. Therefore, it is believed that the DCM solvent would not alter the chemical composition of CRM. Besides, the minor boiling point (<40 ^{o}C) of DCM makes the evaporation easier and minimizes the influence of high temperature on the gel layer. As all components of bitumen are soluble in DCM solution, the absorbed gel layer around the CRM core can be peeled off and dissolved. After 30 min of soaking, the sieve net containing CRM particles was moved out of the solvent. It can be observed from Fig. 2(d) that when the gel layer was removed, the CRM particles lost the gloss of bitumen and became loose particles. The beaker containing gel layer-DCM solutions was then stored in an oven of 45 ^{o}C for 9 hours when no liquid solution is visible. Before the sample preparation for chemical tests, all gel layer samples were placed in a vacuum oven of 45 ^{o}C for 5 hours to eliminate any possible remaining DCM or water. To clarify, the gel layer samples were labeled as G-() and the liquid phase samples were labeled as L-(). The separation methods used in this study are repeatable and provide a novel way to investigate the multiphase system of AR, which can be used in more researches on AR or other modified bitumen using particulate modifiers.

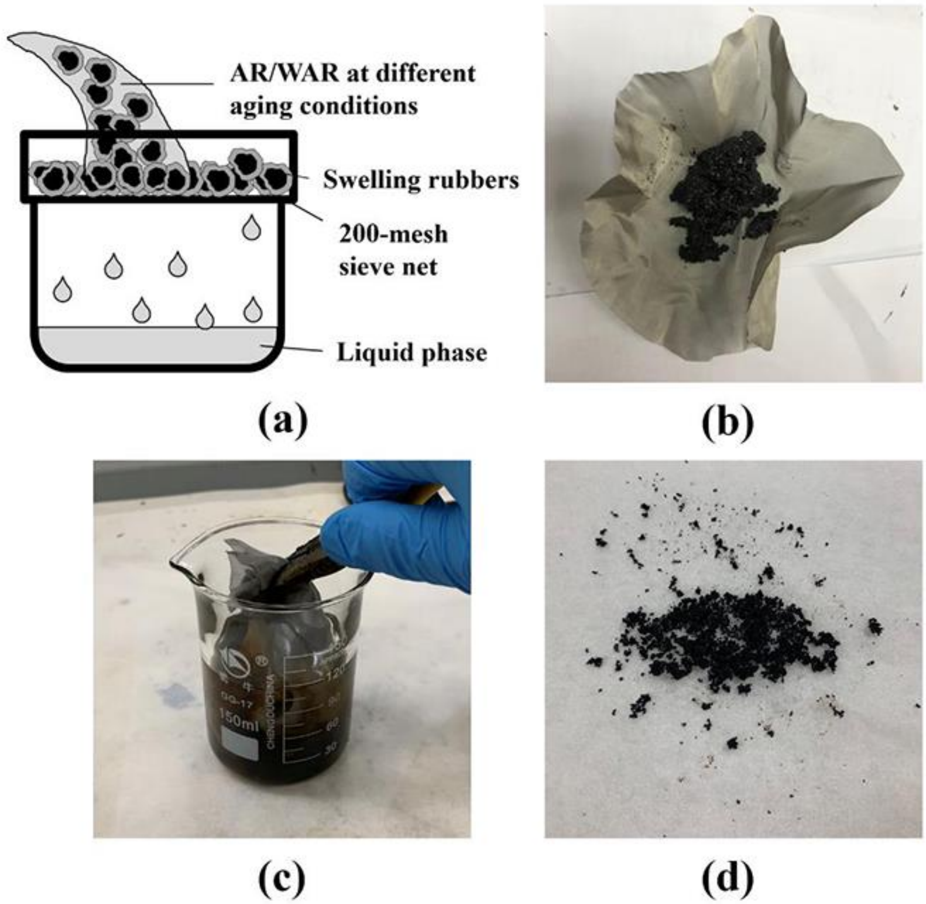

Fig. 2. Separation of binder liquid phase and absorbed gel layer: (a) Separating the binder liquid phase from swelling rubber; (b) Swelling rubber; (c) Extraction of absorbed gel layer; (d) Rubber without absorbed gel layer

2.4 Testing Program

In this study, chemical tests were mainly conducted on the separated phases of AR/WARs to characterize the difference in composition change between the binder liquid phase and gel layer during the aging process. In addition, rheological tests were conducted to monitor the evolution of rheological properties of the rubberized bitumen samples under aging effect. Fig. 3 presents the test scheme for different test samples.

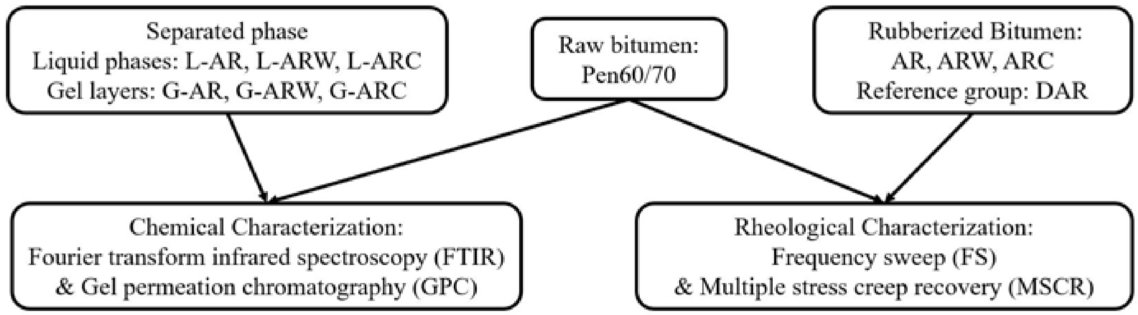

Fig. 3. Test scheme

2.4.1 Fourier-transform infrared spectroscopy (FTIR) test

A PerkinElmer FTIR Spectrometer in attenuated total reflectance (ATR) mode was used to estimate the change of functional groups in asphalt during aging. The wavenumber range is from 4000 to 400 cm^{-1} with a resolution of 4 cm^{-1}. At least five replicates were scanned for each sample at different aging conditions. To quantitively evaluate the effect of aging on different asphalt binders, same baseline correction was performed for all spectra, and the peak areas under a series of specific absorbance bands were integrated for analysis. The carbonyl (C=O) and sulfoxide (S=O) Indexes, which are recognized indicators of bitumen oxidation, were adopted to represent the aging degree (Zhao et al., 2016; Sreeram et al., 2018). The calculations of these two indexes are shown in following equations:

$$I_{C=O}(\text{Carbonyl index}) = \frac{A_{1700/1650}}{A_{ref}} \quad (1)$$

$$I_{S=O}(\text{Sulfoxide index}) = \frac{A_{1030}}{A_{ref}} \quad (2)$$

$$A_{ref} = A_{1700/1650} + A_{1030} + A_{(1375,1455)} + A_{1600} + A_{966} + A_{(2953,2862)} + A_{(863,810,750,720)} \quad (3)$$

where $A_{1700/1650}$ and A_{1030} represent the integrated areas under the carbonyl and sulfoxide peaks, respectively; and A_{ref} is the sum of total considered peak areas for reference (Tarsi et al., 2018).

2.4.2 Gel permeation chromatography (GPC) test

An Agilent 1260 GPC equipped with two chromatographic columns (PLgel 3μm Mixed-E and PLgel 5μm 10^3Å) was used for measuring the molecular weight distribution of different binders.

The temperature of the two columns was 30 ºC. Tetrahydrofuran (THF) solvent was used as the mobile phase with a flow rate of 1 mL/min and an injection volume of 20 μL. The binder sample was dissolved into THF solvent at a concentration about 1.0 mg/mL. The constituents of different molecular sizes in binder were separated by the porous gel particles in columns and eluted in the order from large to small. A refractive index differential (RID) detector was used to record the concentration of the expelled molecules. To quantify the molecular weight distribution of the binder sample, the GPC chromatograms were split into several slices and the area of each slice was integrated. The proportion of a certain molecular size level can be represented by its area ratio (Area%), which was calculated as the area of the corresponding slice divided by the total area (Bowers et al., 2014).

2.4.3 Frequency sweep (FS) test

The rheological tests were carried out by a dynamic shear rheometer (DSR). FS tests were conducted to characterize the viscoelastic properties of the binder samples in the temperature range of 10-60 ºC with an increasing interval of 10 ºC. 25 mm diameter plate was used for 40-60 ºC tests and 8 mm diameter plate was used for 10-30 ºC tests. At each testing temperature, the complex shear modulus and phase angle of the binders at 16 specified frequencies between 0.1-100 Hz were determined. To ensure the binders maintain the linear viscoelasticity, the strain level was controlled at 0.1%. The Williams-Landel-Ferry (WLF) equation (Equation 4) was used for the calculation of shift factors.

$$\log \alpha_T(T) = \frac{-C_1(T-T_{ref})}{C_2+(T-T_{ref})} \quad (4)$$

where $\alpha_T(T)$ is the shift factors; C_1 and C_2 are coefficients of regression; T is the experimental temperature; and T_{ref} is the reference temperature. In addition, a modified Christensen-Anderson-Marasteanu (CAM) model was adopted for fitting the master curves of complex modulus (Equation 5) and phase angle (Equation 6) based on the FS test results. The modified CAM model has been proved to accurately depict the plateau region of phase angle master curve of rubberized asphalt due to the presence of rubber (Wang et al., 2020c).

$$G^* = \frac{G_g^*}{[1+(f_c/f_r)^k]^{\frac{m}{k}}} \tag{5}$$

where G^* represents the complex modulus, Pa; G_g^* is the glass complex modulus as the frequency approaches infinity, Pa; f_r is the reduced frequency, rad/s; f_c is the crossover frequency, rad/s; and k, m are fitting coefficients.

$$\delta = 90I - \frac{90I - \delta_p}{\left\{1+[\frac{\log(f_p/f_r)}{R_d}]^2\right\}^{\frac{m_d}{2}}} \tag{6}$$

where δ is the phase angle, °; δ_p is the value of the inflection point of the phase angle master curve, °; f_p is the location parameter at which δ_p occurs, rad/s; R_d and m_d are fitting coefficients; and $I = 0$ if $f_r > f_p$, $I = 1$ if $f_r \leq f_p$.

2.4.4 Multiple stress creep recovery (MSCR) test

According to AASHTO M332-18, the MSCR test characterizes the rutting resistance for asphalt binder after short-term aging. With the ability to detect the elastic response of binder, this method has also been used to characterize the microstructural changes of polymer modified bitumen with different aging levels (Wang et al., 2020c). Creep loads at different stress levels (0.1 kPa and 3.2 kPa) were applied to the sample in a pattern of 1-second loading and 9-second rest period. Starting with 0.1 kPa, 10 cycles were repeated at each stress level. Samples under different aging conditions (unaged, short-term aged, long-term aged) were all tested using 25mm-diameter plates at 64 ºC. In addition, a 2 mm shear gap was used for rubberized bitumen to eliminate the effect of CRM particles. The non-recoverable creep compliance (J_{nr}) was calculated by Equation 7 for analysis from the average value of 10 cycles at different stress levels.

$$J_{nr} = \varepsilon_{nr}/\sigma \tag{7}$$

where ε_{nr} is the nonrecoverable strain; and σ is the stress level, 0.1/3.2 kPa.

3 Results and Discussion

3.1 Change of liquid phase ratio during aging

As aforementioned, the absorption behavior of rubber converts the raw bitumen into a multiphase system. Fig. 4 shows the liquid phase ratios of the binder samples under different aging conditions, which were calculated by dividing the mass of separated liquid phase by the total mass of the binder. It can be seen that in AR binder, liquid phase ratio slightly decreased after TFO aging but rose significantly during long-term aging. Meanwhile, the wax-based additive further increased the liquid phase ratio after 2 cycles of PAV aging. The liquid phase ratio of ARC had the similar variation trend, but it was relatively lower the others. It should be noted that the liquid phase ratio measured here may not represent the actual phase separation condition of AR at the service temperature. However, the change of liquid phase ratio still implies that the interaction between swelling rubber and asphalt liquid phases were altered during aging, indicating a possible composition exchange between the liquid phase and absorbed gel layer. More discussion is conducted below on how the change of liquid phase ratio is related to the aging resistance of AR/WAR binders in conjunction with other test results.

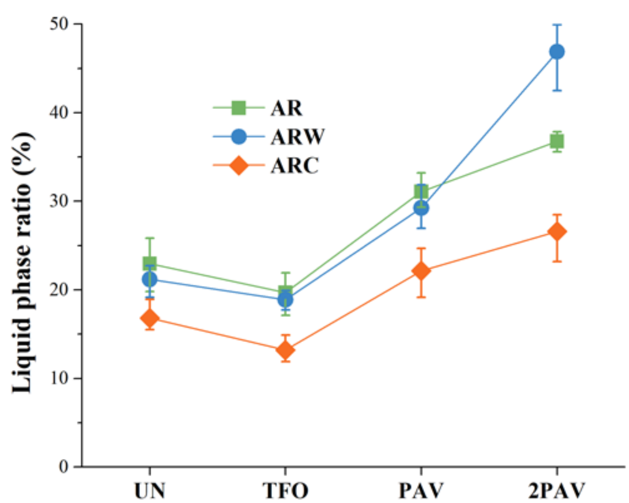

Fig. 4. Variation of liquid phase ratio during aging

3.2 FTIR test analysis

The sulfoxide and carbonyl indexes of each sample were calculated from the FTIR test results to represent their oxidation degree. By comparing the oxidation degree of Pen60/70 and different phases of AR, the effect of adding CRM and rubber absorption can be analyzed. Fig. 5 shows that both indexes increased with aging. In Fig. 5(a), the sulfoxide indexes of L-AR and G-AR are both smaller than those of Pen60/70 after long-term aging, which indicates the better aging resistance brought by the addition of CRM. Previous studies have suggested that the anti-aging effect of CRM could come from the rubber-formed polymer network and the released ingredients like carbon black and antioxidants which hinder the penetration of oxygen into asphalt (Wang et al., 2020c; Ouyang et al., 2006; Wang et al., 2019). On the other hand, Fig. 5(a)&(b) show that the carbonyl and sulfoxide indexes of G-AR are smaller than L-AR under all aging conditions. It implies a lower degree of oxidation for the binder fractions being absorbed in the gel layer. One possible reason is that the polymer network in the gel layer is stronger and could better protect the absorbed light fractions against the attack of oxygen. However, Fig. 5(b) shows that the carbonyl index of L-AR is greater than that of Pen60/70. This phenomenon can be explained by the selective absorption of swelling rubber. The increase of carbonyl peak at 1700 cm^{-1} is well related to the ketone compounds formed in side chains attached to the highly condensed aromatic rings in asphaltenes (Apostolidis et al., 2017). As rubber itself is reluctant to absorb asphaltenes into the gel layer, most of the asphaltenes are left in the liquid phase (Yu et al., 2016). Thus, the larger proportion of asphaltenes in L-AR resulted in the higher carbonyl index.

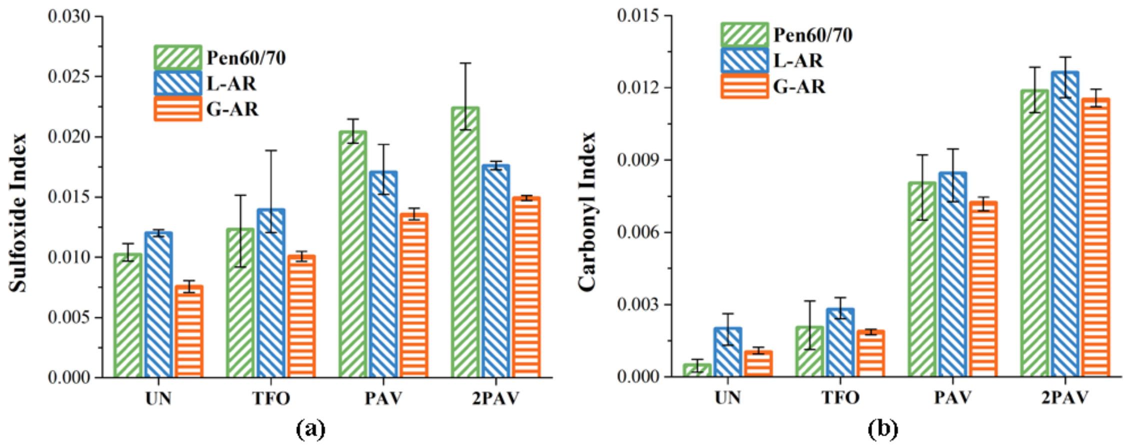

Fig. 5. Evolutions of sulfoxide index and carbonyl index in Pen60/70 and AR during aging: (a) Sulfoxide index; (b) Carbonyl index

When it comes to the evolution of carbonyl and sulfoxide indexes in WARs, the influence of WMA additives on the functional group distribution should be specified based on FTIR curves. Fig. 6 illustrates some critical changes in the FTIR curves of AR and WAR before and after 2PAV aging. The augmentation of sulfoxide peak at 1030 cm^{-1} after long-term aging was detected for all binders, representing the oxidation that happened during aging. In addition, it can be seen that the carbonyl peaks at 1700 cm^{-1} in L-AR and L-ARW arose and became prominent after aging. It indicates that mixing wax-based additive into AR had insignificant effect on its aging-related functional groups. By contrast, the incorporation of chemical additive shifted the carbonyl peak from 1700 cm^{-1} to 1650 cm^{-1}. Unlike the carbonyl group at 1700 cm^{-1} related to the ketone compounds, the carbonyl group at 1650 cm^{-1} is the indicator of amide compounds. It was the fatty amine derivatives and alkylamines in the chemical additive that created this peak in L-ARC (Yu et al., 2020b). More surprisingly, the carbonyl peak at 1700 cm^{-1} was not observed after long-term aging, while the carbonyl peak at 1650 cm^{-1} became more pronounced. One likely explanation is the nitrogen atom is more electronegative than the carbon atom, so the carbon linked to nitrogen is more prone to lose electrons and have oxidative reaction than the carbon linked to carbon. Therefore, the C-N bond in amide compounds reacted more actively with oxygen throughout the aging process, resulting in the bulking up of the carbonyl band at 1650 cm^{-1} instead of that at 1700 cm^{-1}. Besides, it should be noted that the FTIR curves of the liquid phase and gel layer in each binder are overall similar with no obvious change of functional groups.

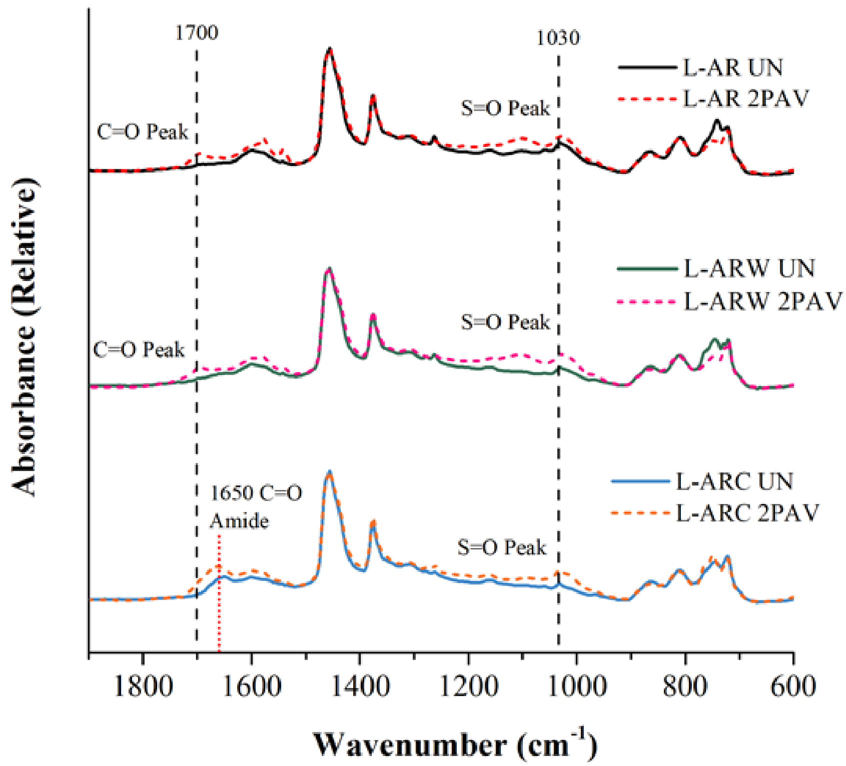

Fig. 6. FTIR spectra of AR and WARs at unaged and after 2PAV aging (Vertical shifts for better comparison)

As shown in Fig. 7(a), the sulfoxide indexes of ARC and ARW both increased with aging. Similar to AR, the lower sulfoxide index of each gel layer compared with their corresponding liquid phase suggests the protective effect of rubber on the absorbed fractions against oxygen. Meanwhile, the lower sulfoxide index of ARC compared with ARW may also derive from the C-N bond in chemical additive which is more appealing to oxygen. On the other hand, Fig. 7(b) shows that the carbonyl indexes of ARC and ARW differed clearly although both ascended with aging. The evolutions of carbonyl index in L-ARW and G-ARW were approximate to that in AR, assuring the limited effect of wax-based additive on the aging properties of AR. However, the chemical additive brought a notable difference to the aging of the carbonyl group in L-ARC and G-ARC. The carbonyl index of ARC was calculated from the peak area at 1650 cm^{-1}, so it has a larger dimension than the carbonyl indexes of AR and ARW. It can be seen that the carbonyl index of G-ARC was higher than that of L-ARC under unaged condition. It means that the swelling rubber was inclined to absorb the chemical additive into its gel layer. The carbonyl index of L-ARC and G-ARC also increased with aging, indicating more carbon atoms linked to nitrogen were oxidized. With a stronger absorption preference towards the amide compounds, the carbonyl index of G-ARC was greater than that of L-ARC throughout the aging process.

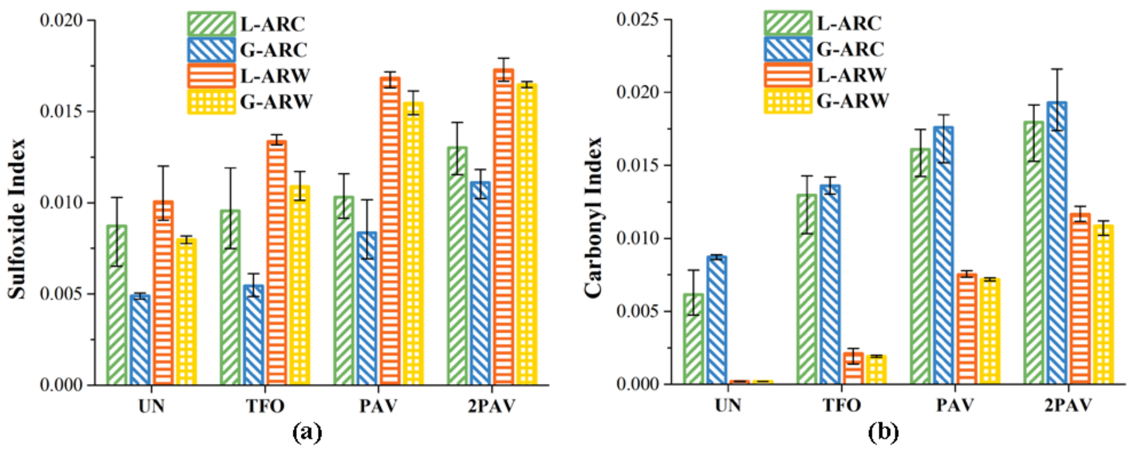

Fig. 7. Evolutions of sulfoxide index and carbonyl index in WARs during aging: (a) Sulfoxide index; (b) Carbonyl index

3.3 GPC test analysis

In this study, GPC analysis was conducted to compare the molecular weight distribution of liquid phases and gel layers in AR/WAR binders during aging. Fig. 8 exhibits the GPC chromatograms of different phases in AR and WARs at unaged and 2PAV aged conditions. For better comparison, the curves were normalized to the peak value and the *x*-axis was converted from elution time to equivalent molecular weight. Meanwhile, the GPC curves were divided into three sections, namely large molecular size (LMS), medium molecular size (MMS), and small molecular size (SMS). As expected, the GPC curves of L-AR and G-AR in Fig. 8(a) present distinct difference under unaged condition, indicating the selective absorption of rubber towards the light fractions of bitumen (Yu et al., 2020b). After 2PAV aging, the curves in LMS section were shifted upwards due to the oxidation of bitumen and the increasing portion of asphaltenes. Besides, the elution point of L-AR was advanced from 4.5 to 4.75, which implies the emergence of some oversized molecules. However, Fig. 8(b) shows that the elution point of Pen60/70-2PAV was only around 4.5. One possible explanation for this is that part of the rubber polymers was degraded and released from the rubber core into the bitumen during aging, increasing the molecular weight of bitumen. From the kinetics point of view, the diffusion of bitumen light fractions into swelling rubber can propel the degradation of rubber polymers (Wang et al., 2020a). The degradation of rubber polymers also brought softening effect to the aged bitumen. It is important to note that in Fig. 8(a) the curve of G-AR still differed from L-AR after 2PAV aging, which verifies the persistent preferential absorption behavior of rubber during aging.

Fig. 8(c) shows that the GPC curves of ARW and their evolution are generally similar to that of AR, but ARW eluted earlier at about 5.0 after 2PAV aging. This phenomenon suggests that the dissolution of rubber molecules was possibly promoted by the incorporation of wax-based additive, corresponding to the greater liquid phase ratio of ARW-2PAV in Fig. 4. By comparison, L-ARC and G-ARC in Fig. 8(d) show the latest elution point around 4.3, which may derive from the surfactant ingredients of chemical additive deagglomerating the large molecules into smaller molecules. With smaller molecular weight, the bitumen was easier to be absorbed by rubber, resulting in the lower liquid phase ratio of ARC in Fig. 4.

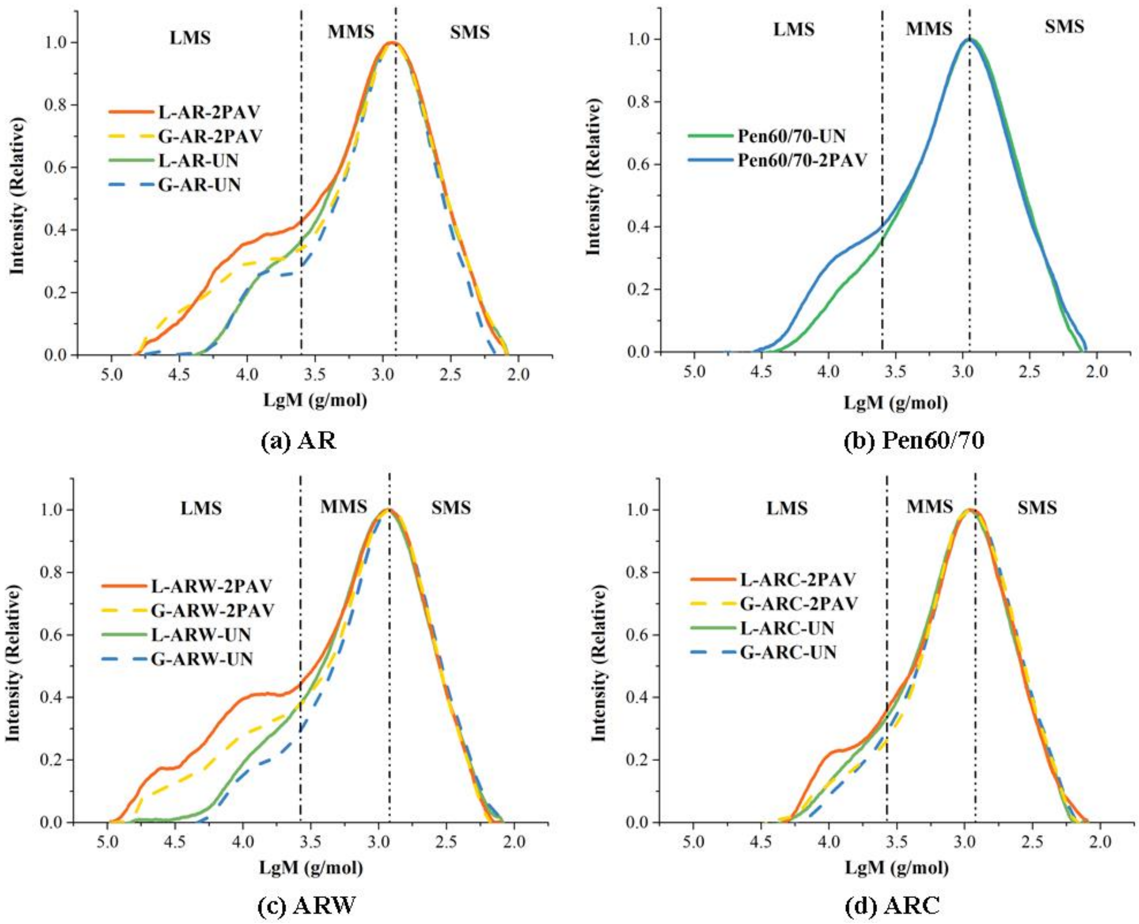

Fig. 8. Evolutions of GPC curves of different binders during aging

To quantify how the absorption behaviors of rubber evolved during aging, the molecular size range of each section and their Area%s in different samples were summarized in Table 2. In general, the aging of bitumen leads to a greater LMS ratio and a lower SMS due to the oxidation and the fractions change inside bitumen. Such tendencies can be found in all samples, including the liquid phases and gel layers. Throughout the whole aging process, the gel layers of AR and WARs kept a higher SMS ratio and a lower LMS ratio than their corresponding liquid phases under different aging conditions, indicating the preservation function of rubber absorption. Rubber was prone to hold the lighter fractions inside the gel-layer, which helped to maintain a relatively softer internal environment around the swelling rubber particles. Simultaneously, part of the large molecular components may be expelled from the gel layer into the liquid phase, resulting in the rise of liquid phase ratio with aging. As swelling rubber performs a dominant role in the performance of AR and WAR, its relatively stable mechanical property may positively affect the aging resistance. In addition, the more rapid growth of LMS ratio in AR and ARW compared with Pen60/70 reveals the dissolution of rubber during aging, and the deagglomeration effect of chemical additive can be assured by the lowest LMS ratio of ARC.

TABLE 2 Evolutions of molecular weight distribution in different binders during aging

Aging Conditions	**LMS (Area%) (> 3953 g/mol)**		**MMS (Area%) (840-3953 g/mol)**		**SMS (Area%) (< 840 g/mol)**	
	Pen60/70		**Pen60/70**		**Pen60/70**	
Unaged	13.20		45.88		40.92	
TFO	14.20		45.42		40.38	
PAV	16.78		44.00		39.22	
2PAV	18.96		44.26		36.78	
	L-AR	**G-AR**	**L-AR**	**G-AR**	**L-AR**	**G-AR**
Unaged	15.00	13.92	45.00	44.77	38.99	41.31
TFO	19.94	15.74	43.63	44.29	36.43	39.97
PAV	24.84	20.55	39.80	41.05	35.36	38.41
2PAV	26.65	22.89	39.78	39.63	33.57	37.48
	L-ARW	**G-ARW**	**L-ARW**	**G-ARW**	**L-ARW**	**G-ARW**
Unaged	13.92	13.16	46.99	43.78	39.09	43.06
TFO	19.11	15.71	43.56	41.76	37.32	42.53
PAV	22.34	18.18	41.59	41.79	36.07	40.04
2PAV	28.76	19.74	39.26	40.74	31.98	39.53
	L-ARC	**G-ARC**	**L-ARC**	**G-ARC**	**L-ARC**	**G-ARC**
Unaged	12.70	9.19	49.05	48.61	38.25	42.19
TFO	12.35	7.96	48.51	47.83	39.13	44.22
PAV	12.55	8.38	48.52	48.44	38.93	43.18
2PAV	14.89	10.26	48.45	47.96	36.66	41.78

3.4 FS test analysis

With a reference temperature of 25 ºC, the complex modulus and phase angle master curves of Pen60/70, DAR, and AR at different aging conditions are drawn in Fig. 9 to compare the evolution of their overall viscoelastic properties during aging. In general, aging came along with the upward movement of complex modulus master curve and the downward movement of phase angle master curve for all three binders, indicating their greater elastic but less viscous behaviors after aging. It can be seen from Fig. 9(a)&(b) that the addition of CRM increased the modulus of raw bitumen at lower frequency region but decreased the modulus at higher frequency region, which represents the better rutting resistance and less brittleness of DAR compared to Pen60/70. The comparison demonstrates that simply mixing CRM into raw bitumen as elastic fillers could moderately improve its rheological properties. However, the obvious gaps between master curves of DAR at different aging states indicate that the aging resistance of raw bitumen was not significantly improved by the simply distributed CRM. By comparison, Fig. 9(c) shows that the master curves of AR at different aging conditions had much narrower gaps between each other, highlighting the anti-aging effect brought by the absorption and dissolution of CRM.

To comprehensively evaluate the role of CRM during aging, the rheological properties of DAR and AR at different aging conditions and frequency regions should be further compared. It can be seen from Fig. 9(b)&(c) that the moduli of AR-UN and AR-TFO at lower frequencies are higher than that of DAR-UN and DAR-TFO. In the early stage of aging, the bitumen matrix was relatively soft, so the swelling rubber particles were more effective than simply distributed CRM in improving the stiffness by reducing the free space inside the binder. However, after the long-term aging, the lower frequencies modulus of DAR increased rapidly while that of AR only had moderate augment. Meanwhile, the modulus of AR at higher frequencies was smaller than DAR throughout the whole aging process. Combined with the findings from FTIR and GPC tests, the less changed rheological properties of AR during aging can be attributed to three different behaviors of swelling CRM: 1) the released polymer chain, carbon black and anti-oxidants from CRM retarded the oxidation of reactive bitumen groups, especially for those were absorbed into the gel layer; 2) the dissolution of rubber polymers during the aging process created a softening effect to partially offset the hardening effect of aging bitumen; and 3) the preservation effect of rubber absorption could keep the mechanical property of swelling rubber relatively stable, so as to improve the aging resistance of whole binder system.

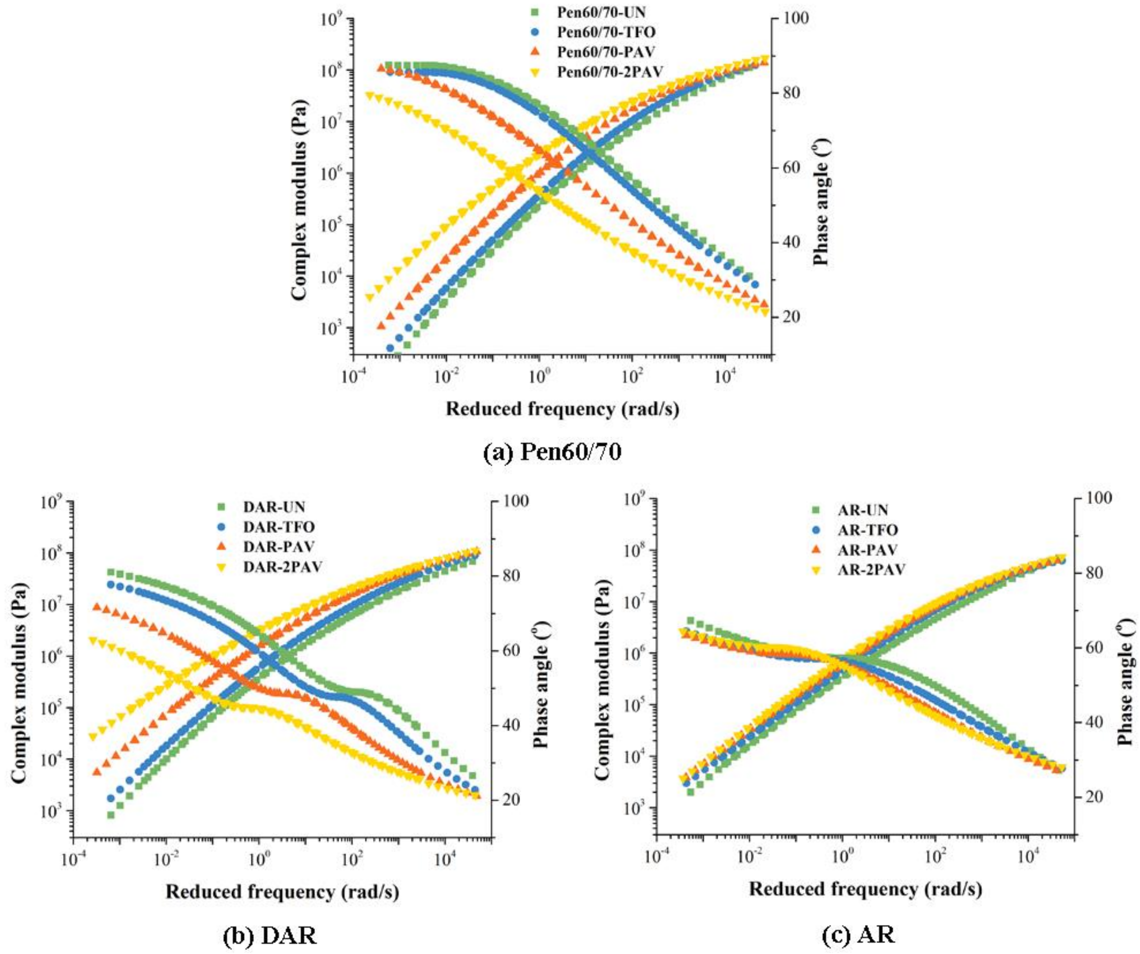

Fig. 9. Evolutions of overall rheological properties of Pen60/70, DAR and AR during aging

When the WMA additives were added, the rheological properties of WARs and their evolution during aging were both affected. As shown in Fig. 10(a), the chemical additive brought a softening effect to AR, so ARC had lower modulus and higher phase angle than AR at unaged condition (Wang et al., 2020d). After TFO and PAV aging, the master curves of ARC shifted more obviously than AR due to the volatilization of the liquid components in chemical additive. Subsequently, ARC became stiffer than AR after 2PAV aging at lower frequencies. It can be attributed to the lower liquid phase ratio of ARC and thus the smaller free space between swelling rubbers. As for ARW, the small intervals between the modulus master curves at different aging conditions indicate its excellent aging resistance, as shown in Fig. 10(b). The modulus of ARW was significantly improved by the incorporation of wax-based additive over the entire frequency range. The phase angle master curves of ARW became disordered at lower frequencies due to the crystallized structure formed by the wax-based additive (Wang et al., 2020d). Thus, the modified CAM model also failed to capture the special trend of phase angle in ARW. With the decrease of frequency, the phase angle ascended first and then descended. The turning point of phase angle refers to where crystallized wax became more proactive than bitumen matrix to dominate the rheological properties of ARW at lower frequencies. Besides, the peak phase angle of ARW decreased and the turning point shifted to lower frequencies after aging because the bitumen matrix became stiffer.

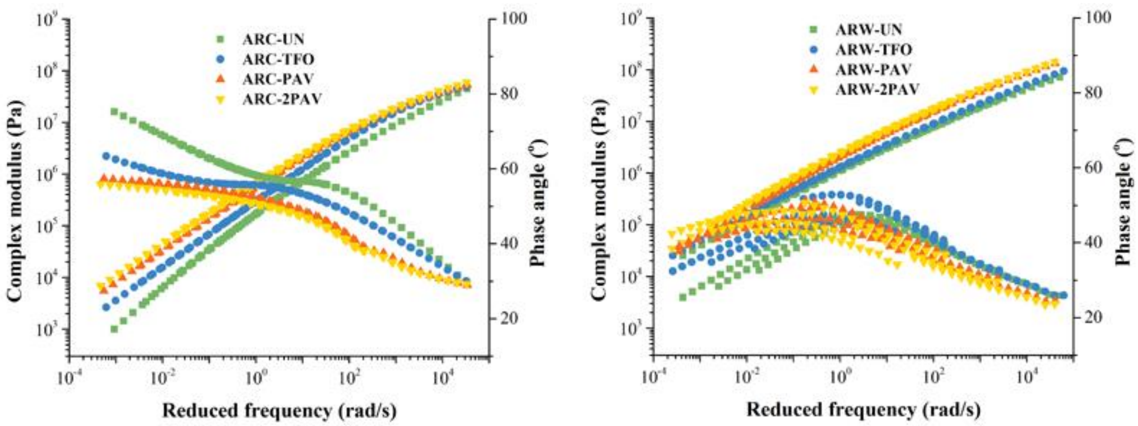

(a) ARC (b) ARW

Fig. 10. Evolutions of overall rheological properties of ARC and ARW during aging

3.5 Analysis on the evolutions of different rheological parameters during aging

To further quantify the effect of rubber absorption and warm mix additives on the aging resistance of bitumen, two rheological parameters, namely the Glover-Rowe (G-R) parameter ($G^* \cdot (\cos\delta)^2 / \sin\delta$) and the J_{nr} at 3.2 kPa were adopted to evaluate the evolution of the rheological properties of each sample during aging. The G-R parameters are derived from the established master curves at the frequency of 0.005 rad/s and temperature of 15 ºC, which are used to characterize the brittleness and ductility of asphalt binder (Mensching et al., 2015). J_{nr} is the result from MSCR tests at 64 ºC that can be used as the indicator of the microstructural changes in asphalt binder during aging. Meanwhile, the change ratios of these two parameters were calculated (Equation 8) to measure the rate of aging.

$$Aging\ rate = \frac{G-R_{Aged}}{G-R_{Unaged}}\ or\ \frac{J_{nr\ unaged}}{J_{nr\ aged}} \tag{8}$$

where $G - R_{Aged}$ and $J_{nr\ aged}$ are the G-R parameter and J_{nr} under TFO, PAV, and 2PAV aging conditions, respectively; and $G - R_{Unaged}$ and $J_{nr\ unaged}$ are the G-R parameter and J_{nr} under unaged condition, respectively.

As shown in Table 3, the G-R parameter increased while J_{nr} decreased with aging, both indicating the stiffening effect of aging on different asphalt binders. The addition of CRM significantly increased the G-R parameters and decreased the J_{nr} of raw bitumen under unaged and TFO conditions, which implies the complex microstructure formed due to the interaction between rubber and bitumen. It should be noted that the cracking resistance of AR and Pen60/70 cannot be evaluated through parallelly comparing their G-R parameters, because this parameter cannot reflect the role of the polymer network in absorbed gel layers to prevent the propagation of microcracks (Wang et al., 2020d). However, it is reasonable to use the aging rates to assess the ability of different binders to restrain the change of their own rheological properties during aging, i.e., the aging resistance. In Table 3, DAR shows a lower aging rate than Pen 60/70, but it is still much larger than AR. It confirms that although the distribution of elastic fillers slightly improved the aging resistance of raw bitumen, the absorption and dissolution of CRM played a more indispensable role during the aging process. As for the WARs, ARC presented a slightly higher aging rate than AR and ARW during the TFO aging and first PAV aging due to the partial volatilization of liquid form chemical additives. The extremely large G-R parameters and low J_{nr} of ARW stemmed from the solid state of wax below its own melting point, manifesting the strong microstructure formed by the wax-based additive. Nevertheless, ARW still maintained excellent aging resistance when the wax-based additive significantly affected its rheological properties. Overall, the incorporation of WMA additives did not compromise the superior aging resistance of AR.

Based on the results, it is suggested that adequate mixing time and temperature should be controlled to ensure the sufficient swelling of rubber, so as to obtain the satisfied aging resistance of AR in field application. Meanwhile, the absorptive capability of rubber should be considered as one of the critical indexes in the rejuvenation of reclaimed AR pavement. The use of WMA additives is feasible because it does not undermine the aging resistance but provides a more environmental-friendly production of AR pavement. Yang et al. (2017) reported that the AR prepared with chemical additive could save up to 14% of fuel comparing to normal AR. A comparative life cycle assessment on the AR pavement with different WMA technologies also showed that the wax-based and chemical additives can significantly decrease the energy consumption during material extraction and production stage (Cao et al., 2019). It should be noted that the selection of WMA additives should be determined according to the actual need. The wax-based additive can be applied to high-temperature regions where a better rutting resistance is needed, and the chemical additive is more suitable in low-temperature regions.

TABLE 3 Evolutions of different rheological parameters and their aging rate

Binder types	**Aging conditions**	**G-R Parameters**	**Aging rate (G-R)**	**J_{nr} (/3.2 kPa)**	**Aging rate (J_{nr})**
Pen60/70	Unaged	0.161	1.000	6.024	1.000
	TFO	0.819	5.077	3.680	1.637
	PAV	11.324	70.160	1.166	5.166
	2PAV	120.605	747.202	0.335	17.982
DAR	Unaged	4.585	1.000	1.617	1.000
	TFO	14.429	3.147	0.616	2.623
	PAV	104.723	22.842	0.274	5.906
	2PAV	387.424	84.504	0.069	23.600
AR	Unaged	18.835	1.000	0.679	1.000
	TFO	29.070	1.543	0.326	2.082
	PAV	40.875	2.170	0.167	4.068
	2PAV	53.391	2.835	0.155	4.115
ARC	Unaged	5.667	1.000	1.398	1.000
	TFO	23.001	4.059	0.582	2.400
	PAV	49.081	8.661	0.108	12.963
	2PAV	63.333	11.176	0.080	18.944
ARW	Unaged	176.0646	1.000	0.205	1.000
	TFO	181.9655	1.034	0.044	4.683
	PAV	277.2484	1.575	0.021	9.542
	2PAV	342.762	1.947	0.020	10.467

4 Conclusions

This study investigated the effect of rubber absorption on the aging resistance of AR and WAR binders prepared with waste tire rubber through chemical and rheological analyses. The following points summarize the major findings of this study:

- The addition of CRM could mitigate the oxidation degree of bitumen, while the bitumen fractions absorbed into the gel layer were even less oxidized, indicating the protective function of rubber absorption.
- Rubber tended to preserve the absorbed light fractions inside the gel layer and expel the heavy fractions into the liquid phase, which maintained the relatively softer environment of the swelling rubber. The stable mechanical property of swelling rubber offset part of the bitumen hardening.
- The rheological analyses revealed that the rheological properties of AR and WAR binders were much less changed than those of base bitumen and DAR. The quantification of aging rates verified the indispensable role of rubber absorption in improving the aging resistance of AR rather than just being distributed elastic filler. Sufficient rubber absorption should be ensured in the production of AR to obtain adequate aging resistance.
- The amide components of chemical additive caused a big difference to the FTIR and GPC results of AR, while the wax-based additive significantly stiffened the binder. However, WMA additives didn't compromise the aging resistance of AR, so the use of WMA additives is recommended for more energy saving and emission reduction.

It is worth noting that all the tests in this study were conducted at binder level. Future studies will be extended to 1) the role of rubber absorption and dissolution during aging at mastic and mixture levels and 2) the recovery of rubber's absorptive capability for the rejuvenation of aged AR biner.

5 Acknowledgments

This work was supported by the Hong Kong Research Grant Council [Project #: 15209920]; Hong Kong Environment and Conservation Fund [ECF Project 84/2017]; and National Natural Science Foundation of China [NSFC 51808228].

REFERENCES

ASTM-D6144, 2009. Standard specification for asphalt-rubber binder. Am. Soc. Test. Mater.

Apostolidis, P., Liu, X., Kasbergen, C., Scarpas, A.T., 2017. Synthesis of asphalt binder aging and the state of the art of antiaging technologies. Transp. Res. Rec.: J. Transp. Res. Board. 2633, 147–153. https://doi.org/10.3141/2633-17.

Bowers, B.F., Moore, J., Huang, B., Shu, X., 2014. Blending efficiency of reclaimed asphalt pavement: an approach utilizing rheological properties and molecular weight distributions. Fuel 135, 63-68.

Cao, R., Leng, Z., Yu, H., Hsu, S.C., 2019. Comparative life cycle assessment of warm mix technologies in asphalt rubber pavements with uncertainty analysis. Resour. Conserv. Recy. 147, 137-144. https://doi.org/10.1016/j.resconrec.2019.04.031

Kabir, S.F., Zheng, R., Delgado, A.G., Fini, E.H., 2021. Use of microbially desulfurized rubber to produce sustainable rubberized bitumen. Resour. Conserv. Recy. 164, 105144. https://doi.org/10.1016/j.resconrec.2020.105144

Lesueur, D., 2009. The colloidal structure of bitumen: Consequences on the rheology and on the mechanisms of bitumen modification. Adv. Colloid. Interfac. 145, 42–82. https://doi.org/10.1016/j.cis.2008.08.011.

Ghavibazoo, A., Abdelrahman, M., 2013. Composition analysis of crumb rubber during interaction with asphalt and effect on properties of binder. Int. J. Pavement Eng. 14(5), 517–530.

Mensching, D.J., Rowe, G.M., Daniel, J.S., Bennert, T., 2015. Exploring low-temperature performance in black space. Road Mater. Pavement https://doi.org/10.1080/14680629.2015.1077015.

Milad, A., Ali, A.S.B., Yusoff, N.I.M., 2020. A review of the utilisation of recycled waste material as an alternative modifier in asphalt mixtures. Civil Eng. J. 6, 42-60. http://dx.doi.org/10.28991/cej-2020-SP(EMCE)-05

Moraes, R., Bahia, H.U., 2015. Effect of mineral filler on changes in molecular size distribution of asphalts during oxidative ageing. Road Mater. Pavement 16, 55–72. https://doi.org/10.1080/14680629.2015.1076998.

Ouyang, C., Wang, S.F., Zhang, Y., Zhang, Y.X., 2006. Improving the aging resistance of styrene-butadiene-styrene tri-block copolymer modified asphalt by addition of antioxidants. Polym. Degrad. Stab. 91(4), 795–804. https://doi.org/10.1016/j.polymdegradstab.2005.06.009.

Presti, D.L., 2013. Recycled tyre rubber modified bitumens for road asphalt mixtures: a literature review. Constr. Build. Mater. 49, 863-881.

Rahbar-Rastegar, R., Daniel, J.S., Dave, E.V., 2018. Evaluation of viscoelastic and fracture properties of asphalt mixtures with long-term laboratory conditioning. Transp. Res. Rec.: J. Transp. Res. Board 2672(28), 503–513. https://doi.org/10.1177/0361198118795012.

Shu, X., Huang, B., 2014. Recycling of waste tire rubber in asphalt and Portland cement concrete: an overview. Constr. Build. Mater. 67, 217-224.

Sreeram, A., Leng, Z., Yuan, Z., Padhan, R.K., 2018. Evaluation of RAP binder mobilisation and blending efficiency in bituminous mixtures: An approach using ATR-FTIR and artificial aggregate. Constr. Build. Mater. 179, 245-253.

Tang, N., Huang, W., Xiao, F., 2016. Chemical and rheological investigation of high-cured crumb rubber-modified asphalt. Constr. Build. Mater. 123, 847-854.

Tarsi, G., Varveri, A., Lantieri, C., Scarpas, A., Sangiorgi, C., 2018. Effects of different aging methods on chemical and rheological properties of bitumen. J. Mater. Civil Eng. 30(3), 04018009. https://doi.org/10.1061/(ASCE)MT.1943-5533.0002206.

Wang, D., Li, D., Yan, J., Leng, Z., Wu, Y., Yu, J., Yu, H., 2018a. Rheological and chemical characteristic of warm asphalt rubber binders and their liquid phases. Constr. Build. Mater. 193, 547-556.

Wang, H., Liu, X., Apostolidis, P., Scarpas, T., 2018b, Rheological behavior and its chemical interpretation of crumb rubber modified asphalt containing warm-mix additives. Transp. Res. Rec.: J. Trans. Res. Board. https://doi-org.ezproxy.lb.polyu.edu.hk/10.1177/0361198118781376

Wang, H., Liu, X., Apostolidis, P., Scarpas, T., 2018c. Review of warm mix rubberized asphalt concrete: towards a sustainable paving technology. J. Clean. Prod. 177, 302-314.

Wang, T., Xiao, F., Zhu, X., Huang, B., Wang, J., Amirkhanian, S., 2018d, Energy consumption and environmental impact of rubberized asphalt pavement. J. Clean. Prod. 180, 139-158.

Wang, H., Lu, G., Feng, S., Wen, X., Yang, J., 2019. Characterization of bitumen modified with pyrolytic carbon black from scrap tires. Sustainability https://doi.org/10.3390/su11061631.

Wang, H., Apostolidis, P., Zhu, J., Liu, X., Skarpas, A., Erkens, S., 2020a. The role of thermodynamics and kinetics in rubber–bitumen systems: A theoretical overview. Int. J. Pavement Eng. https://doi.org/10.1080/10298436.2020.1724289.

Wang, H., Liu, X., Apostolidis, P., Erkens, S., Skarpas, A., 2020b. Experimental investigation of rubber swelling in bitumen. Transp. Res. Rec.: J. Transp. Res. Board https://doi.org/10.1177/0361198120906423.

Wang, H., Liu, X., Apostolidis, P., Van de Ven, M., Erkens, S., Skarpas, A., 2020c. Effect of laboratory aging on chemistry and rheology of crumb rubber modified bitumen. Mater. Struct. 53, 26. https://doi.org/10.1617/s11527-020-1451-9

Wang, H., Liu, X., Van de Ven, M., Lu, G., Erkens, S., Skarpas, A., 2020d. Fatigue performance of long-term aged crumb rubber modified bitumen containing warm-mix additives. Constr. Build. Mater. 239, 117824. https://doi.org/10.1016/j.conbuildmat.2019.117824.

Xiao, F., Punith, V.S., Amirkhanian, S.N., 2012. Effects of non-foaming wma additives on asphalt binders at high performance temperatures. Fuel 94, 144–155.

Yang, X., You, Z., Hasan, M.R.M., Diab, A., Shao, H., Chen, S., Ge, D., 2017. Environmental and mechanical performance of crumb rubber modified warm mix asphalt using Evotherm. J.

Clean. Prod. 159, 346e358.

Yu, H., Leng, Z., Gao, Z., 2016. Thermal analysis on the component interaction of asphalt binders modified with crumb rubber and warm mix additives. Constr. Build. Mater. 125, 168-174.

Yu, H., Zhu, Z., Zhang, Z., Yu, J., Oeser, M., Wang, D., 2019. Recycling waste packaging tape into bituminous mixtures towards enhanced mechanical properties and environmental benefits. J. Clean. Prod. 229, 22-31. https://doi.org/10.1016/j.jclepro.2019.04.409.

Yu, H., Chen, Y., Wu, Q., Zhang, L., Zhang, Z., Zhang, J., Miljković, M., Oeser, M., 2020a. Decision support for selecting optimal method of recycling waste tire rubber into wax-based warm mix asphalt based on fuzzy comprehensive evaluation. J. Clean. Prod. 121781. https://doi.org/10.1016/j.jclepro.2020.121781.

Yu, H., Leng, Z., Zhang, Z., Li, D., Zhang, J., 2020b. Selective absorption of swelling rubber in hot and warm asphalt binder fractions. Constr. Build. Mater. 238, 117727. https://doi.org/10.1016/j.conbuildmat.2019.117727.

Yu, H., Zhu, Z., Leng, Z., Wu, C., Zhang, Z., Wang, D., Oeser, M., 2020c. Effect of mixing sequence on asphalt mixtures containing waste tire rubber and warm mix surfactants. J. Clean. Prod. 246, 119008. https://doi.org/10.1016/j.jclepro.2019.119008.

Zhao, X., Wang, S., Wang, Q., Yao, H., 2016. Rheological and structural evolution of SBS modified asphalts under natural weathering. Fuel 184, 242–247. https://doi.org/10.1016/j.fuel.2016.07.018.